Engineering Fracture Mechanics, 1972, Vol. 4, pp. 717–736. Pergamon Press. Printed in Great Britain

METHOD OF ANALYSIS AND PREDICTION FOR VARIABLE AMPLITUDE FATIGUE CRACK GROWTH†

THEODORE R. PORTER

Engineer, Research & Engineering Division, Aerospace Group, The Boeing Company, M/S 40–25, P.O. Box 3999, Seattle, Washington 98124, U.S.A.

Abstract—Fatigue crack growth behavior of structure subjected to variable amplitude loading is very complex. Both the truncation and the load sequence have been shown to have a significant influence on the test results because of the load level interaction effects. To understand these interaction effects and the possible influence they can have on the results obtained a test program was performed. Fatigue crack growth tests were conducted on the program using 7075-T6 and 2024-T3 aluminum and titanium 6Al-4V mill anneal.

Using the test data, an analysis method was developed. In this analysis method the crack growth rate is evaluated for each load cycle using a modification of the fracture mechanics correlation technique. The crack growth for each cycle was evaluated as a function of the stress intensity factor excursion with a correction factor for the maximum and minimum peak stress levels in the test spectrum. The fatigue crack growth correction for the peak stresses in the spectrum is given as a growth rate correction factor r. The relationship for r, is termed the 'fatigue crack growth rate interaction model'.

For verification, the interaction model was applied to test data from spectrum loading tests. The correlation obtained for the example, indicated that the model properly predicts the interaction effects and its use could significantly improve the accuracy of crack growth life calculations for programmed spectrum tests.

INTRODUCTION

CURRENT criteria for military and commercial aircraft require prediction of fatigue performance of aircraft structure. For example, in the Air Force ASIP Program[1], a fatigue test article is required to establish service life. The new requirements presently being developed in MIL-A-008866A (USAF)[2] includes fatigue crack growth prediction as an integral part of the service life analysis. These analyses and tests require an understanding of the performance of the structure when subjected to service loadings. Unfortunately, testing time and cost require that the representative loading spectrum must be truncated to an acceptable number of cycles. In addition, load sequence and stress levels must be selected and applied in a repeated programmed manner.

Both the truncation and the load sequence have been shown to have a significant influence on the test results because of the load level interaction effects. It is therefore necessary to understand these interaction effects and the possible influence they can have on the results obtained from different, but still representative of service, test spectra.

This paper presents a method of correlating fatigue crack growth behavior under variable amplitude loading. The method presented can be used for predicting fatigue crack growth behavior of structure subjected to repeated programmed loading. These predictions are applicable to spectrum load tests representative of full scale fatigue tests. It is anticipated the results presented for the crack growth behavior also can be utilized in the development of methods that will explain and predict the observed behavior.

†Presented at the Symposium on Fracture and Fatigue at the School of Engineering and Applied Science, George Washington University, Washington, D.C., May 3–5, 1972.

DISCUSSION

The estimation of fatigue behavior of structure subjected to variable amplitude loading is a complicated procedure. This complication results from the interaction effect of varying amplitude stress levels on the fatigue crack growth.

Figure 1 presents Boeing test data that demonstrates the influence of high stress levels on subsequent crack growth rates. In the case presented, a 7075-T6 panel was

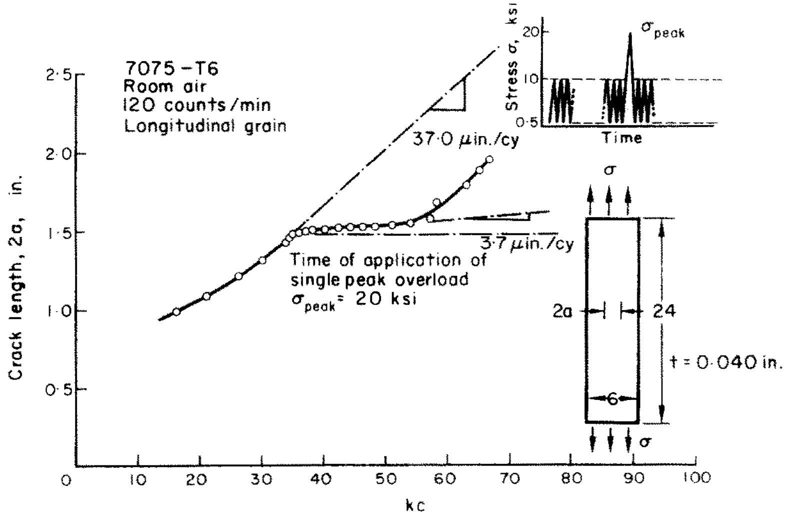

Fig. 1. Single peak overload test data.

cycled with constant amplitude loading. The maximum and minimum stresses were 10 and 0·5 ksi respectively. When the crack reached a length of 1·5 in., a single load cycle was applied with a maximum stress of 20 ksi. Cycling was then continued at the initial stresses. As shown in the figure, the crack growth rate for the subsequent cycling was reduced by an order of magnitude. This influence was observed for over 20,000 cycles.

Similar behavior was observed for repeated spectrum loading. Smith[3] tested center-cracked Ti 8A1–1V–1Mo panels where a high peak load was applied once in a 30-cycle block. The crack growth results are shown in Fig. 2. As shown, the specimen life was extended by the application of the overload cycles, the longest life corresponding to the highest level of overload applied.

The averaged crack growth rate for this data is presented in Fig. 3 as a function of the fracture mechanics parameter K. The K value determined for the baseline (σ_1) stress peak. The lowest average rate of crack growth corresponded to the test with the largest peak overload. These results are replotted in Fig. 4 where the average growth rate is shown as a function of the ratio of overload stress to the baseline level. A trend is presented of decreasing growth rate with increasing stress overload.

For analysis purposes it is assumed that the crack propagates at the baseline stress (σ_1), at a reduced rate while the growth corresponding to the application of the overload (σ_2) stress cycle is not influenced by the variable spectrum. That is, the growth rate for σ_2 is evaluated from constant amplitude test data (no load interaction). The crack growth at the baseline stress (σ_1) in the spectrum (29 cycles) was then found for the

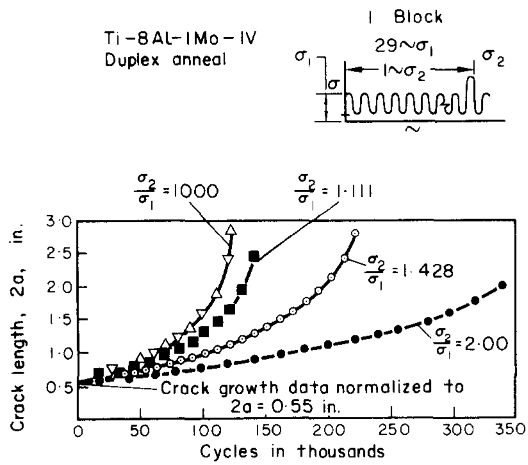

	No.	σ_1/σ_2	σ_2/σ_1	σ_1 ksi	σ_2 ksi
△	C−1	1·0	1·000	14·98	14·98
▽	E−1	1·0	1·000	14·98	14·98
■	D−1	0·9	1·111	14·98	16·66
○	B−1	0·7	1·428	14·98	21·40
●	A−1	0·5	2·00	14·98	29·00

σ_{min} = 1·52 ksi
f = 6 counts/sec

Fig. 2. Influence of peak overload stress on programmed block crack growth.

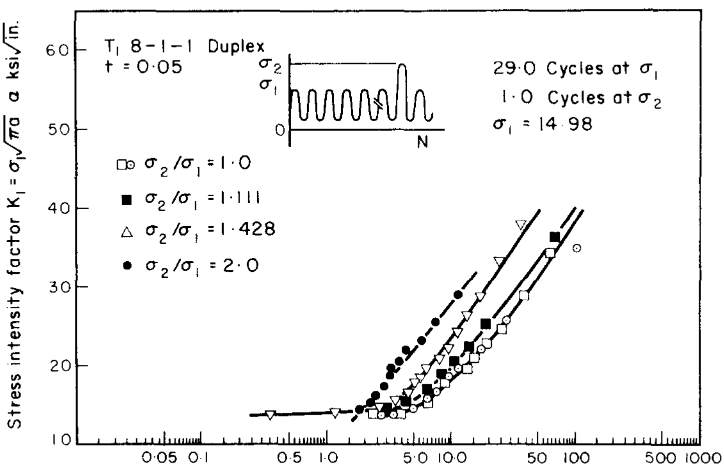

Fig. 3. Influence of peak overload stress on programmed block crack growth rate.

tests by subtracting the growth for the peak overload (σ_2) from the observed total spectrum growth. The resultant estimated growth at σ_1 is illustrated in Fig. 5 as a function of the ratio σ_2/σ_1.

The results shown in Fig. 5 were normalized by taking the ratio of the crack growth rate estimated at σ_1 to the crack growth from constant amplitude data for the same K_1

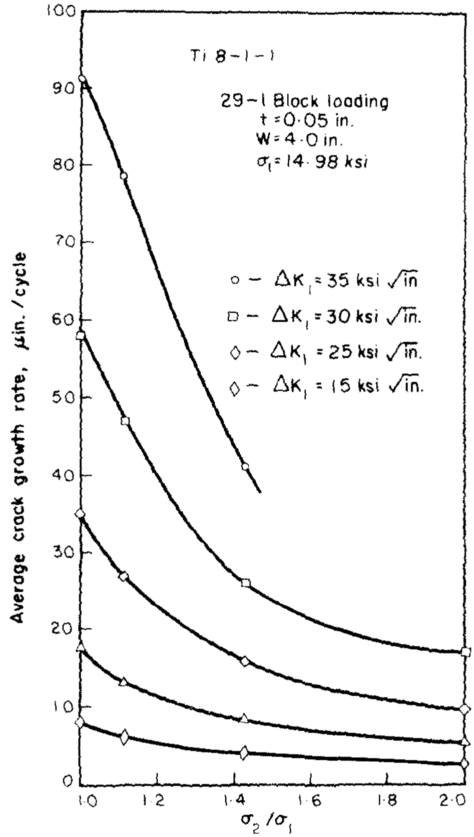

Fig. 4. Influence of peak stress on average crack growth rate.

level. This ratio denoted as r and termed the fatigue crack growth rate reduction factor is shown in Fig. 6 as a function of σ_2/σ_1. The test data point from the results presented in Fig. 1 for the single peak overloading is also plotted. The results shown in the figure demonstrate a trend that can be used for correlation and prediction.

This method given in Fig. 6 shows considerable promise but several questions are raised. These concern:

(1) the influence of mean stress on the growth rate reduction factor r;
(2) the crack growth rate reduction factor when there is more than one overload cycle;
(3) the influence of material;
(4) block size effect;
(5) the influence of the magnitude and sequence of minimum stresses in the spectrum.

A test program was designed to answer some of these questions. The tests were conducted by Boeing Wichita in support of Commercial Airplane Group, Fatigue and Failsafe Research. The test program had four sections:

(a) the effect of repeated peak stresses;
(b) the effect of peak cycle sequence;
(c) the effect of block size;
(d) the effect of peak stress level.

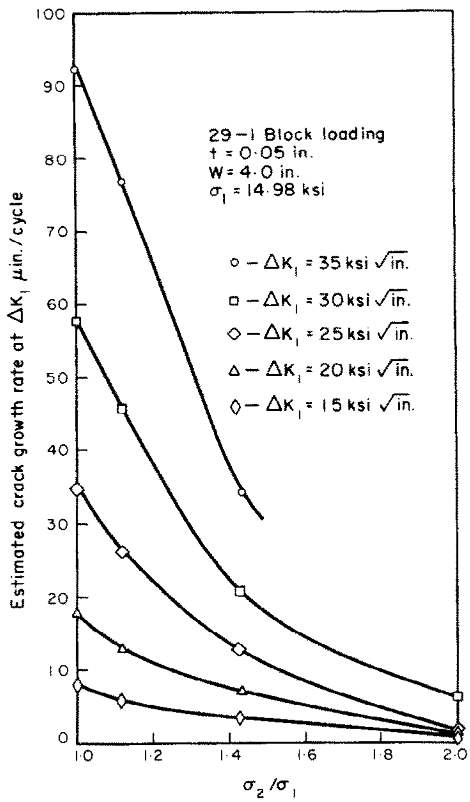

Fig. 5. Influence of peak stress on crack growth rate at σ_1.

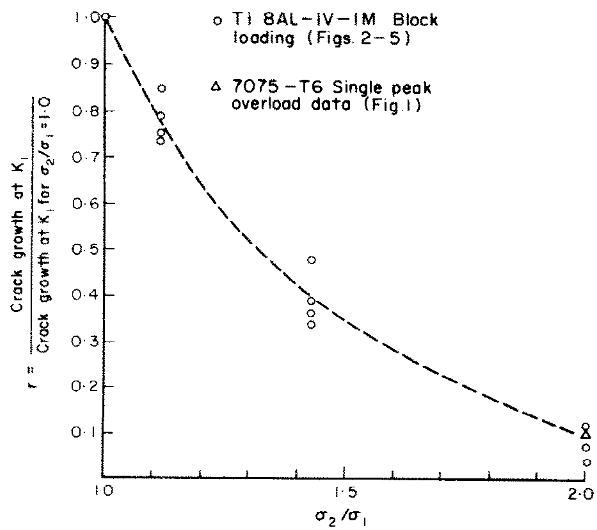

Fig. 6. Influence of peak stress on crack growth rate reduction factor.

Section (b) included mean stress and minimum peak stress effects. The tests were performed on 12 × 36 inch, transverse grain, 0·16 in. thick panels. Materials were 7075-T6, 2024-T3, and Ti 6A1-4V mill anneal.

The test data from the program is presented in Figs. 7–16. The results show similar trends as previously presented, i.e. the crack growth from spectra that contain high load levels produced net reductions in the growth rates.

Figure 7 presents test data showing the cyclic lives with variation in the number of overload cycles. In the block with 50 baseline cycles, it requires 10 overload cycles to produce the same growth rate as the baseline constant amplitude test required. Figure 8 presents the same test data relating load spectra to crack length rather than cycles. in this figure it can be seen that the 60-cycle spectrum containing 10 overloads is only slightly more damaging than the basic 50-cycle spectrum with no overloads.

Figures 9–12 give the results of tests with variable spectrum size. In all cases there was only one overload cycle per spectrum. These results indicate that the maximum life was realized when only a minimum number of overload cycles were applied per spectrum. The same trends are shown for the three tested materials. Presenting the data as a function of number of spectra as in Fig. 10, for 7075-T6 indicates that a significant portion of the crack growth in the tests occurred at the baseline stress.

Figure 13 shows results for 7075-T6 similar to those given in Fig. 2 for Ti 8A1-1V-1Mo. There is a difference, however, in that the large increase in life obtained at $\sigma_2/\sigma_1 = 2{\cdot}0$ when compared to $\sigma_2/\sigma_1 = 1{\cdot}5$ was not found in the 7075-T6 tests.

The results shown in Fig. 14 illustrate test data that include minimum peak stresses. In addition, the influence of load sequence (max–min or min–max) was investigated. The results indicated that the minimum stress tends to cancel the effect of the peak overload; with the greatest cancellation effect if the minimum immediately follows the

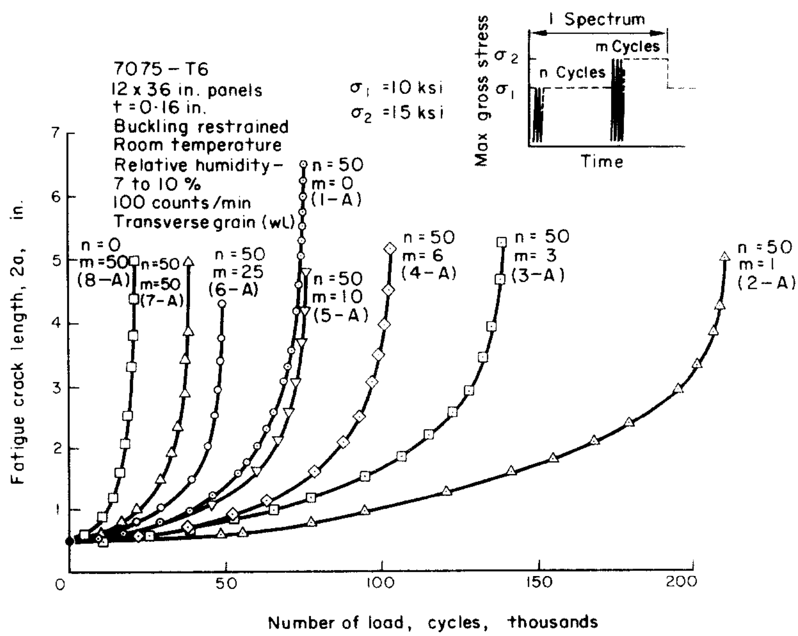

Fig. 7. Crack length vs. cycles behavior of 7075-T6 panels with variable overloads.

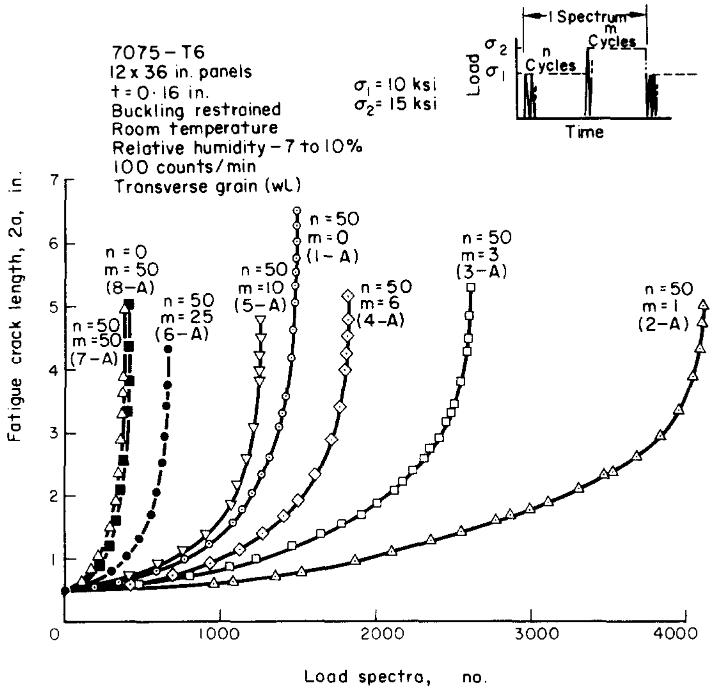

Fig. 8. Crack length vs. spectra behavior of 7075-T6 panels with variable overloads.

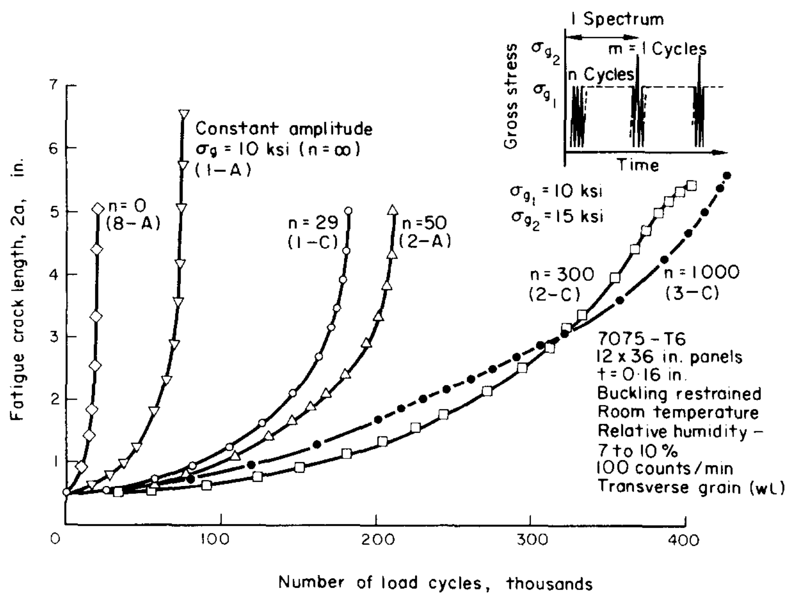

Fig. 9. Crack length vs. cycles behavior of 7075-T6 panels with variable block size.

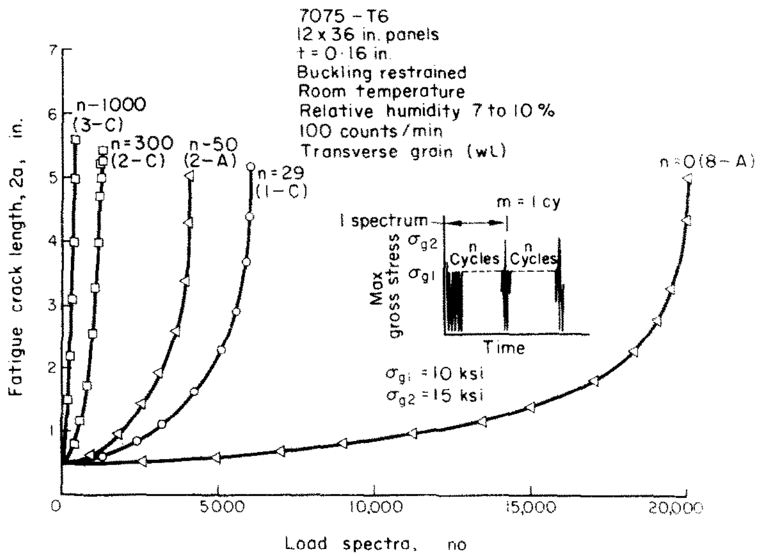

Fig. 10. Crack length vs. spectra behavior of 7075-T6 panels with variable block size.

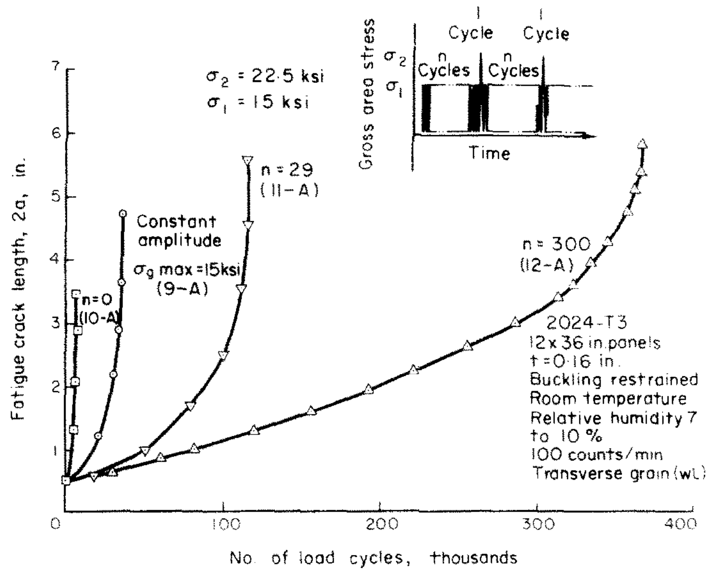

Fig. 11. Crack length vs. cycles behavior of 2024-T3 panels with variable block size.

peak overload. Figures 15 and 16 show data for 2024-T3 and Ti6A1-4V that also illustrates the load order effects.

For purposes of analysis the fatigue crack growth rate reduction factors (r) were evaluated for the test data. Table 1 lists these r factors. These factors were calculated for the σ_{prop} stress levels in the test spectrum, i.e. the baseline stress level in the spectrum.

Using this data a correlation technique was developed. This technique is presented

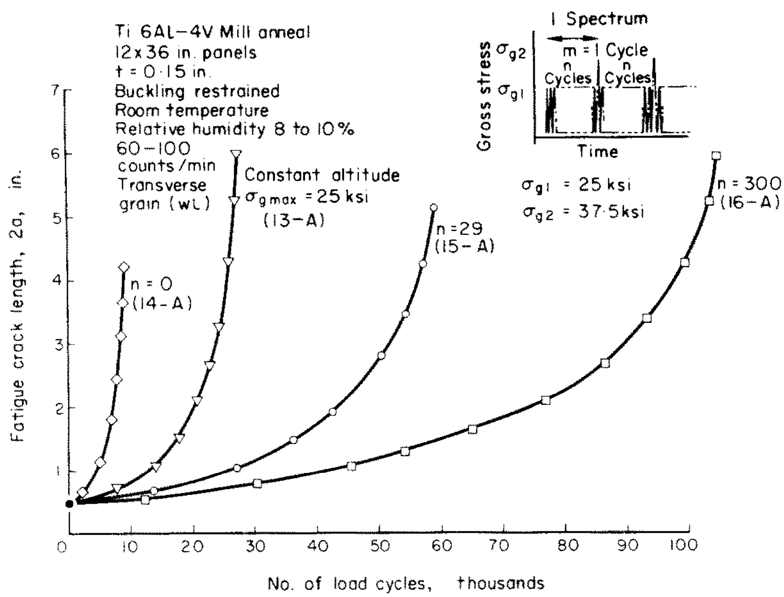

Fig. 12. Crack length vs. cycles behavior of Ti 6A1–4V panels with variable block size.

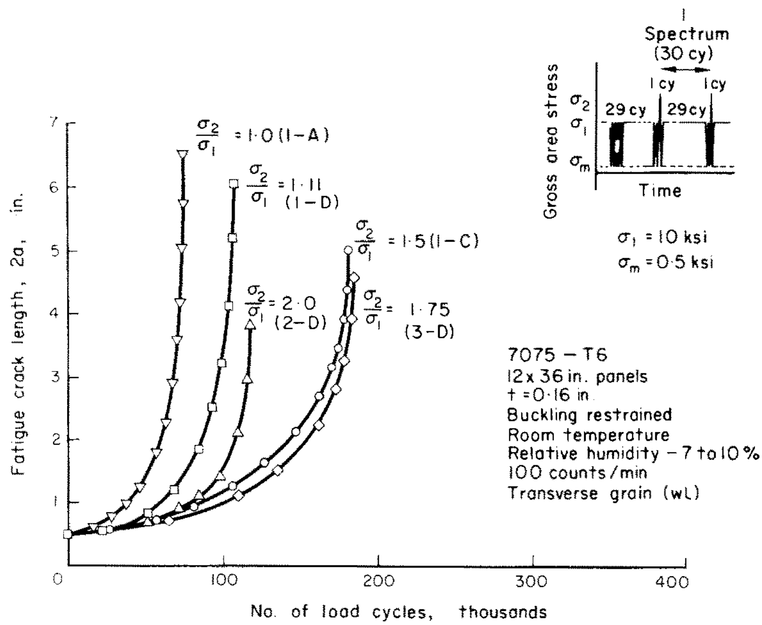

Fig. 13. Crack length cycles behavior of bare 7075-T6 aluminum alloy with variable overload stress.

in Fig. 17 where r is related to the ratio of the total stress excursion in the spectrum divided by the difference between the minimum stress in spectrum and the baseline stress. The results from Table 1 are presented in the figure along with the data given in Fig. 6. The analysis line shown is the same as that drawn in Fig. 6 and represents the fatigue crack growth rate interaction model used in this report.

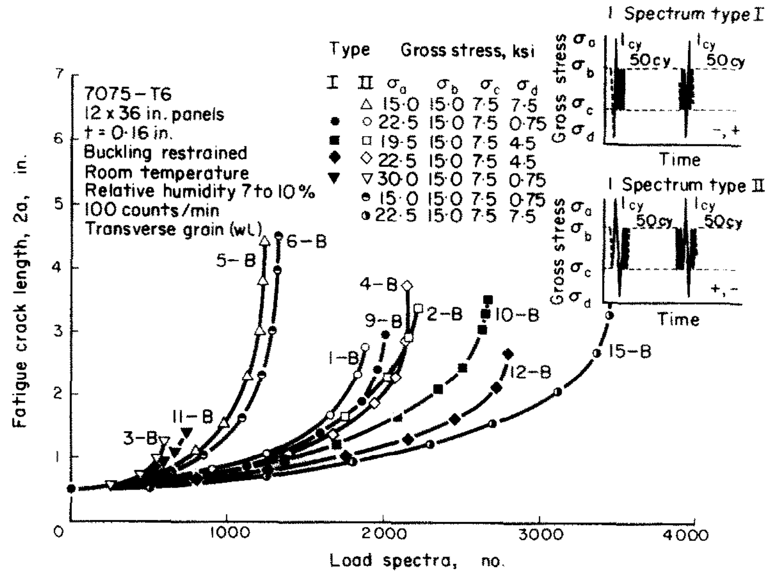

Fig. 14. Influence of peak cycle sequence on crack growth in 7075-T6.

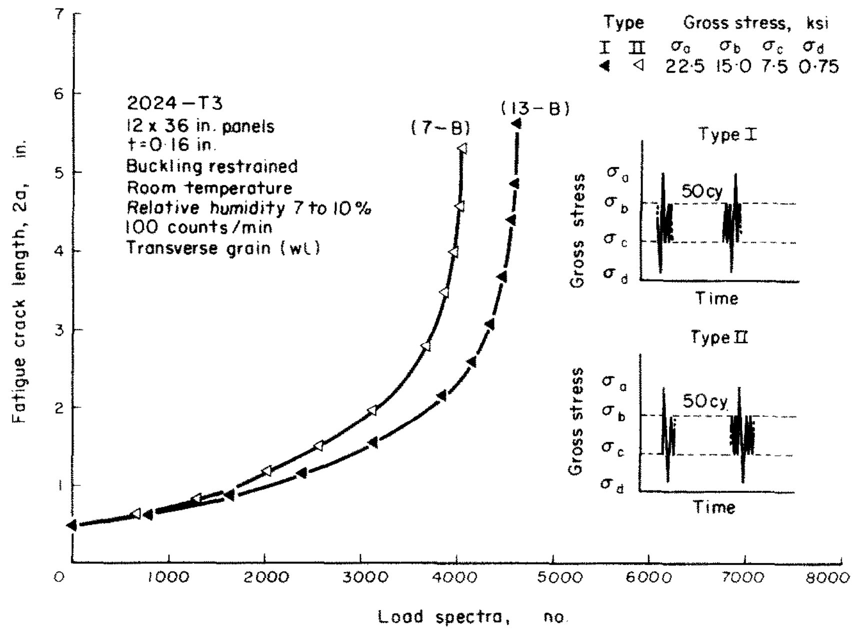

Fig. 15. Influence of peak cycle sequence on crack growth in 2024-T3.

Figure 18 presents the correlation between the interaction model and the test data given in Table 1 for variable stresses. As can be seen, the interaction model gives a good fit of the data and presents the correct trends.

Figure 19 compares the test results and the interaction model with variable block size. A good fit of the data is provided although there is some error. It is possible there

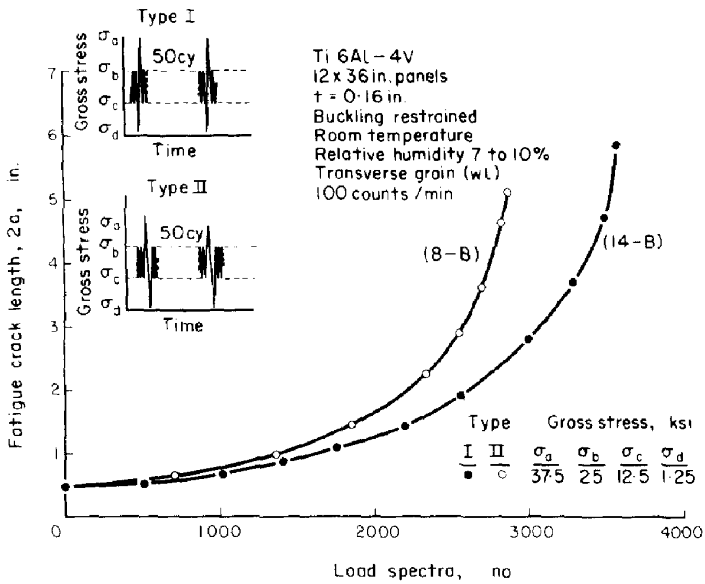

Fig. 16. Influence of peak cycle sequence on crack growth in Ti 6Al-4V.

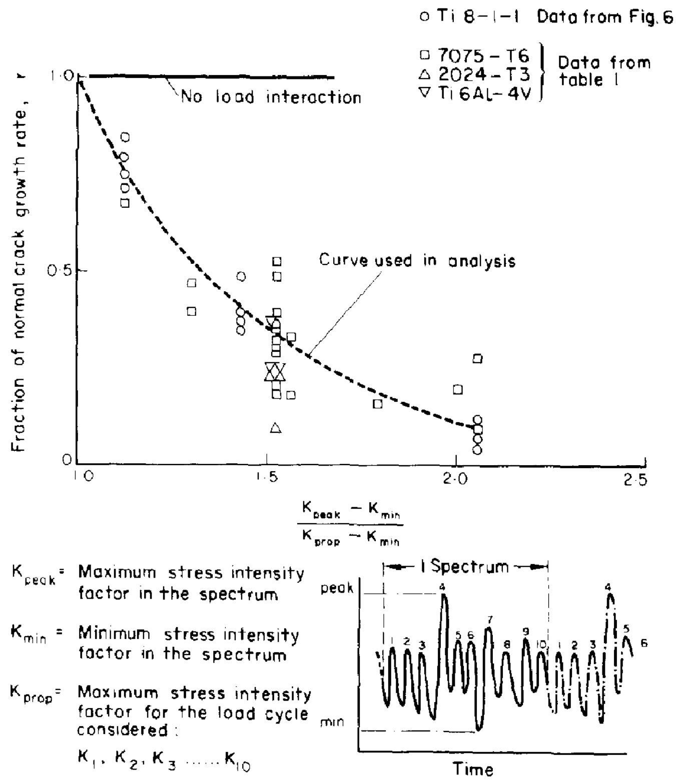

Fig. 17. Fatigue crack growth rate interaction model.

Table 1. Fatigue crack growth rate reduction factors for test data

Test	Material	n	m	σ_{PROP} (σ_b)	σ_C (σ_c)	σ_{PEAK} (σ_a)	σ_{MIN} (σ_d)	r
1-a	7075-T6	50	0	10	0·5	15	0·5	1·0
2-a		50	1					0·29
3-a		50	3					0·37
4-a		50	6					0·39
5-a		50	10					0·48
6-a		50	25					0·52
7-a		50	50					0·36
8-a		0	50					
9-a	2024-73	50	0	15	0·75	22·5	0·75	1·0
10-a		0	50					
11-a		29	1					0·24
12-a		300	1					0·09
13-a	Ti 6Al-4V	50	0	25	1·25	37·5	1·25	1·0
14-a		0	50					
15-a		29	1					0·37
16-a		300	1					0·25
1-b	7075-T6	50	1	15	7·5	22·5	0·75	0·35
2-b						19·5	4·5	0·39
3-b						30·0	0·75	0·28
4-b						22·5	4·5	0·33
5-b						15·0	7·5	1·0
6-b						15·0	0·75	0·85
7-b	2024-T3					22·5	0·75	
8-b	Ti 6Al-4V			25	12·5	37·5	1·25	
9-b	7075-T6			15	7·5	22·5	0·75	0·32
10-b						19·5	4·5	0·47
11-b						30·0	0·75	0·10
12-b						22·5	4·5	0·18
13-b	2024-T3					22·5	0·75	
14-b	Ti 6Al-4V			25	12·5	37·5	1·25	
15-b	7075-T6	50	1	15	7·5	22·5	7·5	0·18
1-c		29	1	10	0·5	15·0	0·5	0·30
2-c		300	1					0·19
3-c		1,000	1					0·19
1-d		29	1			11·1		0·67
2-d		29	1			20·0		0·20
3-d		29	1			17·5		0·16

is a trend reflected by the data presented in Fig. 19, which could be the result of crack growth variations during the block. However, there is insufficient data at this time for verification.

In the interaction model the influence of the peak cycle sequence was neglected. Peak cycle sequence is recognized as a parameter that could be included in the analysis for completeness, but at this time these effects are considered secondary (when compared to the stress magnitude effects). As shown in Fig. 18, the interaction model provides a close fit to both loading orders justifying this approximation.

As a check of this model, test data from [4] was analyzed. In this case crack growth behavior under spectrum loading is predicted using the developed analysis method. The tests in this reference are repeated block spectrum loadings, but were more complex than those previously studied herein with the interaction model. Figure 20 presents

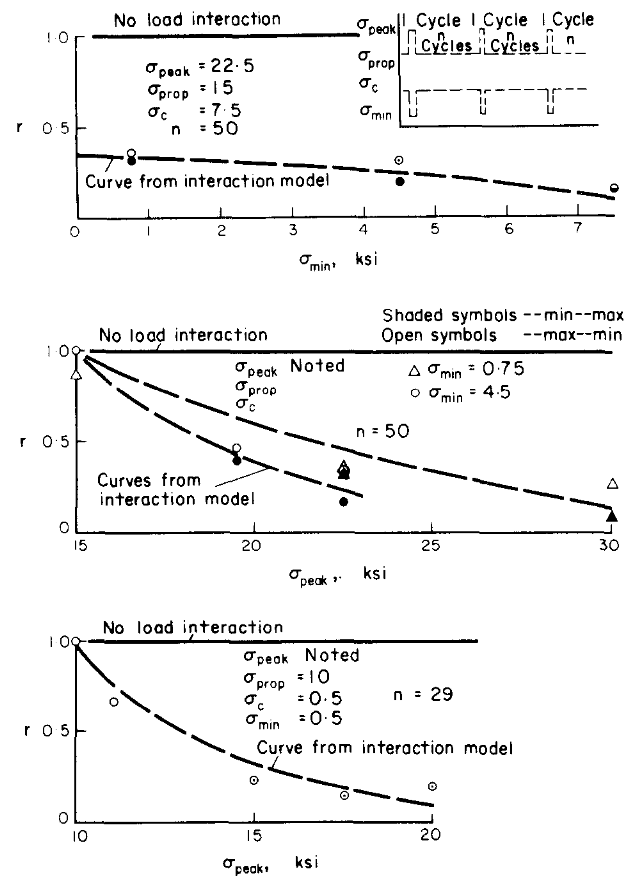

Fig. 18. Comparison at test data and interaction model for variable stress.

the spectrums considered. The test data used was generated with 2024-T3 transverse grain, 0·16 in. thick panels.

Estimates were made of the crack length versus cycles behavior of the panels from constant amplitude data and the interaction model. The basic crack growth data used in the predictions is illustrated in Fig. 21 which was adjusted for the proper β by the curve given in Fig. 22.

A comparison of the growth rates between the analysis and the test data for three selected spectrums is shown in Fig. 23. Two analysis lines are presented: one using the interaction model from Fig. 17, and the other assuming no interaction.

The crack length cycles behavior was estimated for each of the test spectrums with the aid of a computer using a Boeing program. Estimates made with and without use of the interaction model are given in Table 2. For visibility, the results were presented as shown in Fig. 24 where the results of both methods of calculation for each of the test spectrums are compared.

As can be seen in Fig. 24, the correlation between the test and the analysis using the interaction model is quite close; while without using the interaction analysis for some of the spectra, the error was quite large. This indicated that load interaction effects were significant for these particular spectra. These spectra (P6–P11) had variable maximum

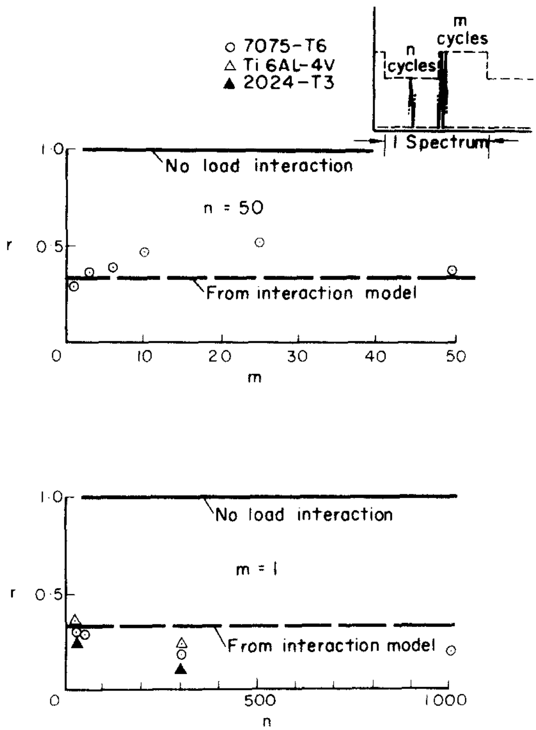

Fig. 19. Comparison of test data and interaction model for variable block size.

Table 2. Estimated cyclic life for 2024-T3 test panels

Test spectrum	Crack growth range (2a in.)	Test life (spectra)	Life estimate using basic data (spectra)	Life estimate using interaction model (spectra)
P1	0·5 to 6·0	4950	4970	4970
P2	0·5 to 6·0	5330	4970	4970
P3	0·5 to 6·0	3630	3670	3670
P4	0·5 to 6·0	1875	1835	1835
P5	0·5 to 6·0	3605	3670	3670
P6	0·5 to 6·0	10,775	6230	10,450
P7	0·5 to 6·0	11,900	6930	12,400
P8	0·5 to 6·0	3860	2690	3770
P9	0·5 to 6·0	3700	2690	3770
P10	0·5 to 6·0	2553	2200	2510
P11	0·5 to 2·893	7900	4540	7050
P12	0·5 to 6·0	5060	4940	5210
P13	0·5 to 2·405	2680	2500	2540

stresses and where the stress cycles with their maximum below σ_{peak} contributed to a significant portion of the crack growth. Spectrums that had a constant maximum (P1–P5) or those that the majority of the cycles were at σ_{peak} (P12 and P13) did not demonstrate the interaction effects as would be expected.

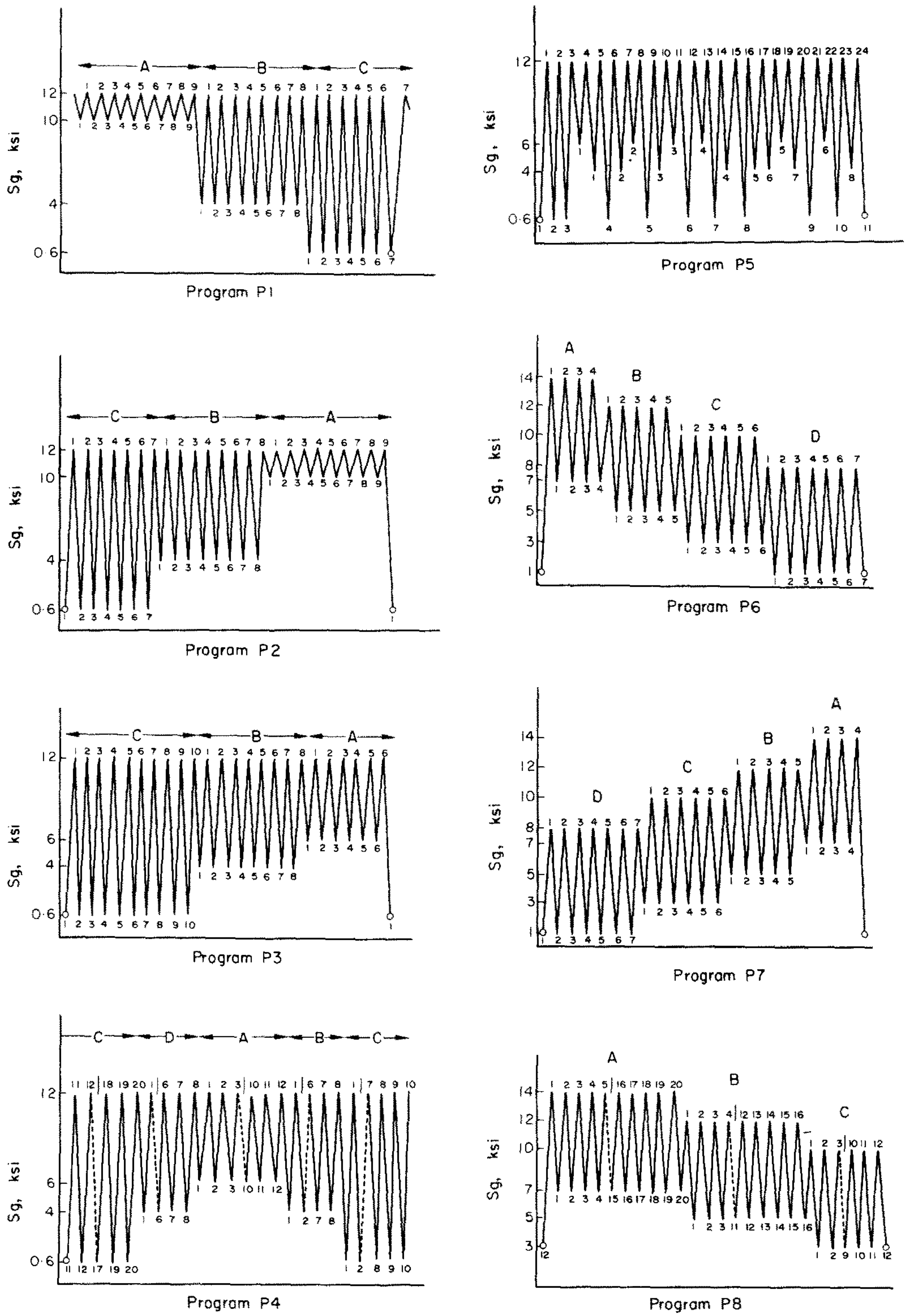
Sg, ksi
Program P1
Program P2
Program P3
Program P4
Program P5
Program P6
Program P7
Program P8

Fig. 20.

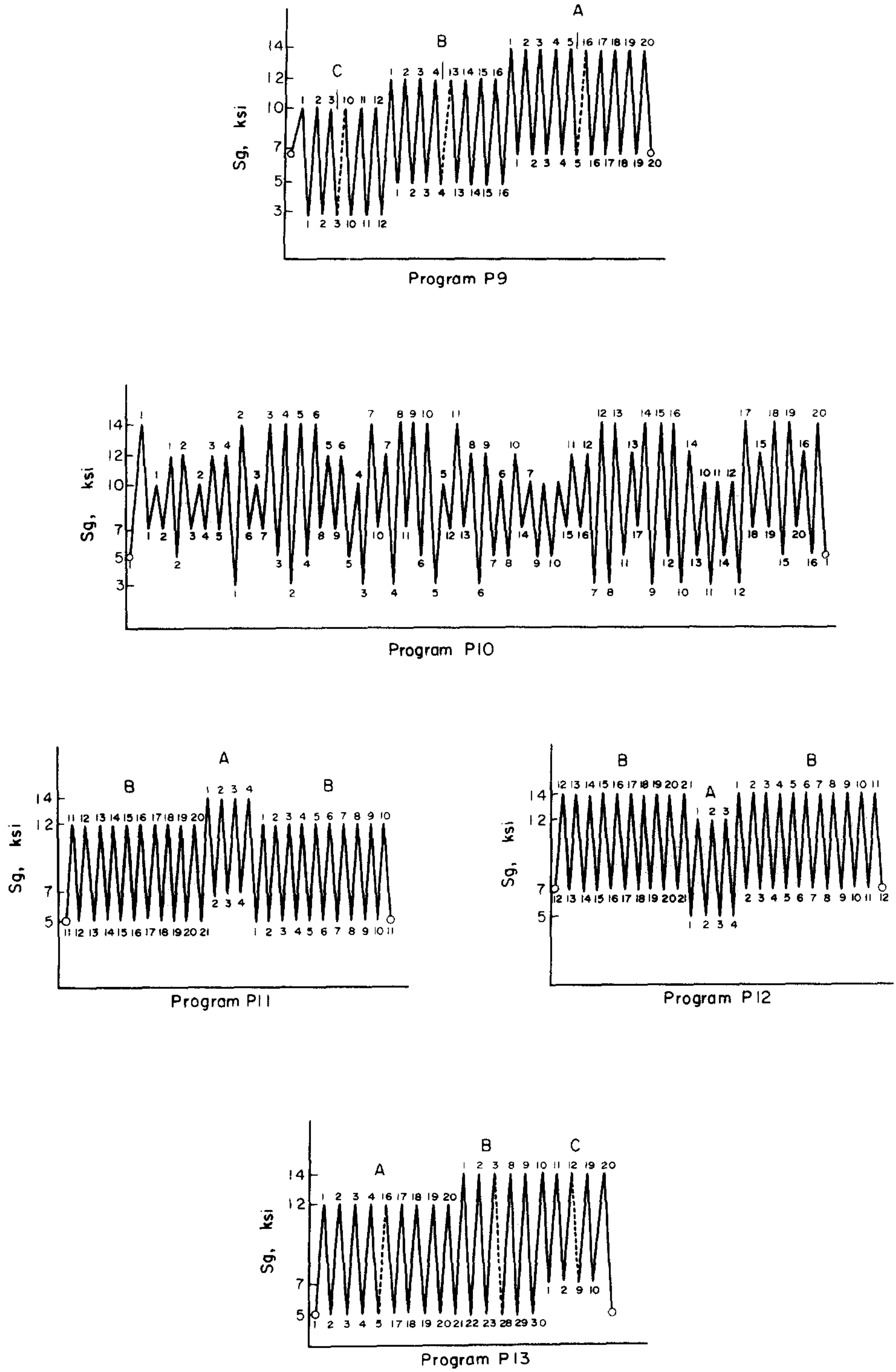

Fig. 20. Test spectra used for example.

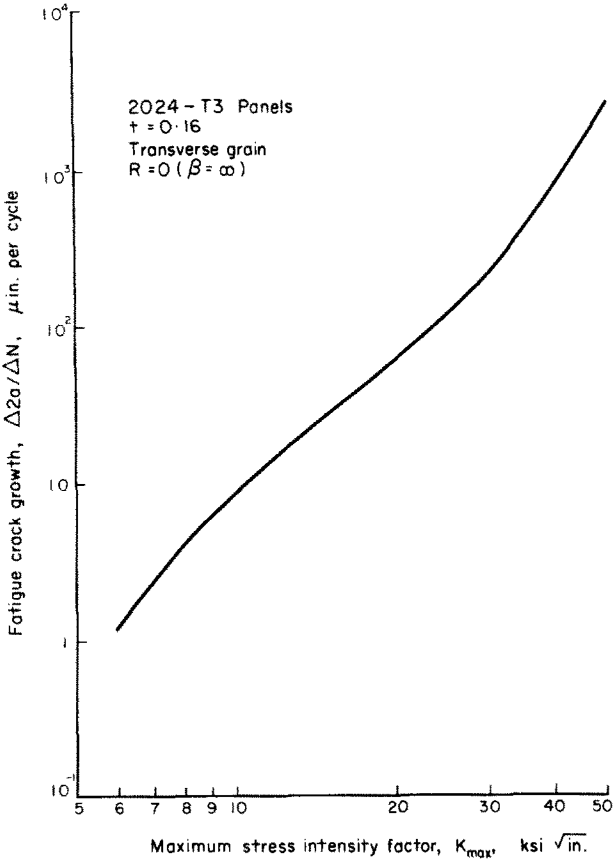

Fig. 21. Basic crack growth rate relationship for 2024-T3 transverse grain.

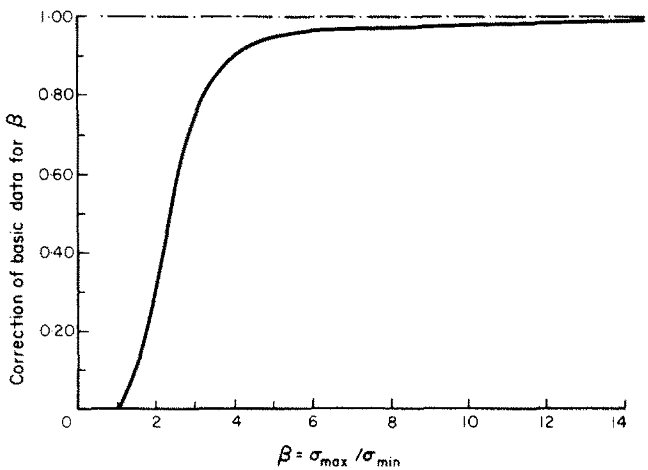

Fig. 22. Influence of the stress ratio (β) on the fatigue crack growth rate.

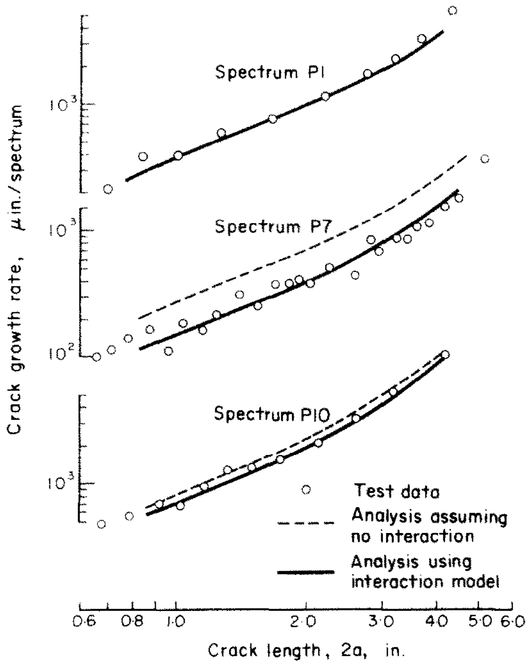

Fig. 23. Comparison of crack growth rates for analysis and test data.

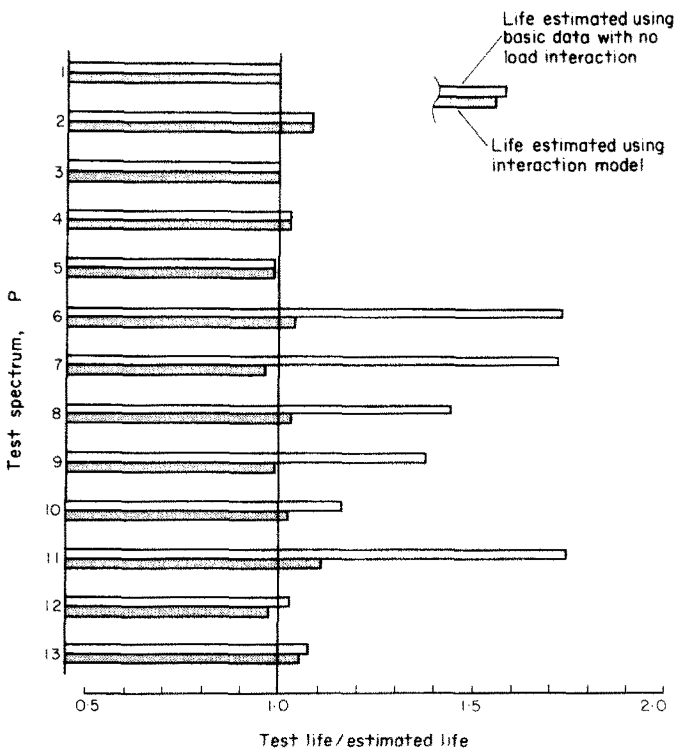

Fig. 24. Comparison of test life to estimated life for 2024-T3 panels.

It should be noted that material was not considered to be a variable in these analyses. The consistency of the results indicated that this is a reasonable assumption. The single peak overload tests were with 7075-T6, the data from [3] was for Ti 8Al–1V–1Mo duplex anneal, the test data in the development program was primarily for 7075-T6 with limited studies on 2024-T3 and Ti 6Al–4V and the data used from [4] in the verification was for 2024-T3.

The interaction model presented was developed for crack growth rates, but another means of application is considered. The cycles required for a crack growth increment for variable amplitude loading can be estimated by using a Minor's rule approach. That is:

$$\sum_{i=1}^{k} \frac{ni}{Ni} = 1$$

where

k = number of steps in spectrum;
ni = number of applied cycles at ith stress;
Ni = life to growth the crack over the increment at the ith stress.

Using the interaction model this can be modified to

$$\sum_{i=1}^{k} \frac{ri\,.\,ni}{Ni} = 1$$

where

ri = crack growth rate reduction factor from the interaction model for the ith stress.

This approach requires that the damage rate (in this case, crack growth) is the same function of fractional life for all stresses. Fatigue crack growth studies indicate this is only approximately true.

The interaction model presented, though demonstrating close correlation with test data, needs further extension and verification. Some of the areas that need to be explored include:

(1) The influence of compression stresses in the spectrum. All of the data considered here was developed with tensile stress only. The effects of the compressive cycle representative of the G-A-G cycle must be considered.
(2) Crack growth for other crack configurations such as cracks from holes, wedge force loaded cracks, edge cracks and surface flaws.
(3) The extension of the method for more general loading rather than repeated blocks.
(4) Determine the influence of plane stress–plane strain modes on crack growth retardation. The majority of the analyses presented in this report were developed for tests that started in plane strain conditions due to the low stresses. The crack growth changed to plane stress for the terminal part of the tests. Some of the scatter experienced in the results could be due to this fracture mode transition.
(5) A basic study of the mechanisms involved. This would include an elastic–plastic analysis of the crack tip where the residual stresses would be considered.

REFERENCES

[1] H. M. Wells Jr. and Troy T. King, Air Force Aircraft Structural Integrity Program. Technical Report ASD-TR-66-57 (May 1970).
[2] MIL-A-8866A (USAF) Airplane Strength and Rigidity Reliability Requirements, Repeated Loads and Fatigue (1971).
[3] S. H. Smith, Random Loading Fatigue Crack Growth Behavior of Some Aluminum Alloys. *ASTM STP* **404** (1968).
[4] J. C. McMillan and R. M. N. Pelloux, Fatigue Crack Propagation Under Programmed and Random Loads, BSRL Document D1-82-0558 (1966). (Also *ASTM STP* **415**.)

(*Received* 31 *March* 1972)